Spline Curve Matching with Sparse Knot Sets: Applications to Deformable Shape Detection and Recognition

Sang-Mook Lee and A. Lynn Abbott
Electrical and Computer Engineering
Virginia Tech
Blacksburg, VA 24061, USA
{lsmook, abbott}@vt.edu

Neil A. Clark and Philip A. Araman
SRS-4702, USDA Forest Service
Blacksburg, VA 24060, USA
{nclark, paraman}@fs.fed.us

Abstract **- Splines can be used to approximate noisy data with a few control points. This paper presents a new curve matching method for deformable shapes using two-dimensional splines. In contrast to the residual error criterion [7], which is based on relative locations of corresponding knot points such that is reliable primarily for dense point sets, we use deformation energy of thin-plate-spline mapping between sparse knot points and normalized local curvature information. This method has been tested successfully for the detection and recognition of deformable shapes.**

I. INTRODUCTION

Curve matching is one of the fundamental tasks in computer vision and has been used to detect and recognize two- or three-dimensional (2D or 3D) objects [22]. Because of its importance, several approaches have been proposed in pursuit of finding an efficient and general curve-matching algorithm [3,10,14,15,16,17,21]. The detection and recognition of non-rigid, deformable curves (or shapes) are particularly well suited to curve-matching methods [5,12,17], and active contour models [18] called "snakes" have been popular for over a decade for modeling and detecting deformable curves in a plane. Among them, B-spline snakes [19] have good potential to be extended into computer-aided geometric modeling and database query. In contrast to their utility for detection purposes, however, B-spline curve representations have rarely been used for curve recognition mainly because of the non-uniqueness of spline parameters [9].

Addressing this non-uniqueness in their pioneering work, Cohen et al. [7] used B-spline knot-point matching for curve classification and recognition. In order to account for affine invariance, they estimated the underlying affine transformation between two curve representations by utilizing moment invariants, and aligned the curves by undoing the transformation [16]. A similar approach is presented in [15], in which both affine-invariant features and B-spline object curves are used for coarse-to-fine matching. However, both approaches have dealt only with affine transformed objects, still leaving in doubt their capability to deal adequately with deformable objects. Furthermore, these approaches used oversampled spline knot points and/or other features to minimize negative effects due to point mismatches.

Motivated by the need to develop a general (especially B-spline based) curve matching algorithm that works on affine transformed objects, as well as on deformable objects, we present a new approach that incorporates deformable mapping and geometric characteristics (strain energy) of spline curves. Our approach operates with small knot sets, and avoids the need for oversampling. A thin plate spline (TPS) model [4] is used in order to extract the deformable mapping parameters between two sets of corresponding points determined by a match matrix method [10] combined with deterministic annealing. Similar point correspondence problems are addressed in [1,6]. A major difference of our point-correspondence method compared to others is that, when constructing the match matrix, geometric information of curves is incorporated at accompanying points in addition to distances. The result is that good matching results are often obtained even with sparse point sets.

Based on the point correspondences that are found, strain energy is calculated to evaluate dissimilarity for each corresponding pair of curve segments. Strain energy is often used as an internal constraint of snakes [18]. Here, however, a mean strain energy is used, which is normalized according to arc length. Along with the deformation energy that is computed when the point correspondence is considered, the strain energy is incorporated into our cost function for curve matching.

Section 2 overviews spline curve representation and estimation, especially for closed curves, and section 3 addresses point correspondence problem and deformation energy. A new matching cost function is formulated in section 4, and demonstrations of the method are presented in section 5. Section 6 concludes the paper.

II. B-SPLINE CURVE ESTIMATION

As a widely used function approximation tool, splines have been extensively used in computer aided geometric design and computer graphics. They have also proven to be useful for curve representation in computer vision and image analysis applications [2,13,15].

0-7803-7906-3/03/$17.00 ©2003 IEEE.

A. B-Spline Representation of Curves

Given a set of knots $\{t_0 < t_1 < \cdots < t_g\} \subset [t_0, t_g] \subset R$, an *n*-degree B-spline function $N_i^{n+1}(t)$ over $[t_i, t_{i+n+1}]$ is defined with the concept of divided difference [9],

$$N_i^{n+1}(t) = (t_{i+n+1} - t_i) \sum_{j=0}^{n+1} (t_{i+j} - t)_+^n \Big/ \prod_{\substack{l=0 \\ l \neq j}}^{n+1} (t_{i+j} - t_{i+l}), \quad (1)$$

where $(x-c)_+^n$ has value $(x-c)^n$ if $x \geq c$, and is otherwise 0. The set of B-splines, denoted $\{N_i^{n+1}(t)\}_{i=0}^{g-n-1}$, have following properties: positive for all *t*, local support, and partition of the unity property. The B-splines are C^{n-1} continuous at the knots, and any C^{n-1} planar curves $\mathbf{f}(t)$ over $[t_n, t_{g-n}]$ has a unique representation

$$\mathbf{f}(t) = [x(t) \;\; y(t)] = \sum_{i=0}^{g-n-1} \mathbf{c}_i N_i^{n+1}(t), \quad t \in [t_n, t_{g-n}], \quad (2)$$

where $\mathbf{c}_i = [c_i^x \;\; c_i^y]$ are now points in 2D, called control points.

To describe closed curves, Flickner et al. [13] have constructed a periodic spline basis by extending the knot sequence, $\{\tilde{t}_i\}_{i=-\infty}^{\infty}$ with $\tilde{t}_i = t_{i \bmod g}$, and accordingly the basis functions by

$$\widetilde{N}_i^{n+1}(t) = \sum_{j=-\infty}^{+\infty} N_{i+jg}^{n+1}(t) \quad (3)$$

where $N_{i+jg}^n(t) = N_i^n(t - g(t_g - t_0))$. The basis still satisfies the above properties. A closed spline curve is then represented as

$$\mathbf{f}(t) = [x(t) \;\; y(t)] = \sum_{i=0}^{g-1} \mathbf{c}_i \widetilde{N}_i^{n+1}(t), \quad t \in \mathbb{R}. \quad (4)$$

B. Least-Squares Spline Curve Fitting

Given a periodic set of knots $\{\tilde{t}_0 < \tilde{t}_1 < \cdots < \tilde{t}_{g-1}\}$, a least-squares spline fit $\hat{\mathbf{f}}$ of *N* data points should minimize

$$\delta = \|\mathbf{v} - \mathbf{E}\mathbf{c}\|^2, \quad (5)$$

where $\mathbf{c}$ is a $g \times 2$ coefficient vector of control points, and $\mathbf{E}$ is a linearly independent $N \times g$ matrix with whose element is $E_{ij} = \widetilde{N}_j^{n+1}(t_i)$. The vector $\mathbf{v}$ is a representation of the data points and is given by

$$\mathbf{v} = [\mathbf{x} \;\; \mathbf{y}] = \begin{bmatrix} x(t_0) & \cdots & x(t_{N-1}) \\ y(t_0) & \cdots & y(t_{N-1}) \end{bmatrix}^T \quad (6)$$

with its parameterization $t_i = t_0 + i(t_g - t_0)/N$. Usually the number of data points is much greater than the number of knots. Here, the parameterization t_i is obtained by the uniform (equidistant) parameterization under the assumption of completely connected boundary data. However, a chord length parameterization method [11] is used in practical situation to cope with the cases that some boundary points are missing, because it preserves the geometry of data points.

Then, the least-squares solution of (5) to find the coefficient vector $\mathbf{c} = [\mathbf{c}_0^T, \cdots \mathbf{c}_{g-1}^T]^T$ is

$$\hat{\mathbf{c}} = \arg\min \|\mathbf{v} - \mathbf{E}\mathbf{c}\|^2 = (\mathbf{E}^T\mathbf{E})^{-1}\mathbf{E}^T\mathbf{v}. \quad (7)$$

Consequently, the fitted spline curve corresponding to the estimated control points is given by $\hat{\mathbf{f}} = [\hat{\mathbf{x}} \;\; \hat{\mathbf{y}}] = \mathbf{E}\hat{\mathbf{c}}$.

Determining the number of knots and their locations, known as the free-knot problem, is a much harder problem to which there currently exists no general optimal solution, though there are several proposed practical techniques. Recent research has addressed this problem from a statistical point of view [8,12].

For the simplicity of the implementation, a practical technique is adopted, by which the number of knots is iteratively increased based on fitting error calculation. Starting with a minimum number of uniformly distributed knots, a new knot is inserted in every iteration until the fitting error tolerance is satisfied. Knot location is determined by selecting a point that causes maximum fitting error. Hausdorff distance between $\mathbf{v}$ and $\hat{\mathbf{f}}$ is used for the error calculation. One constraint used in locating knots is to avoid both multiple or extremely close knots that may disrupt smoothness of the fitted spline curves. Figure 1 shows examples of spline curve fitting. With a few knot points, the splines approximate object boundaries to a given error bound. Only cubic splines (n = 3) is considered throughout the paper.

III. SPARSE KNOT POINTS CORRESPONDENCE

Finding point correspondence is a fundamental task in curve matching and recognition. It is particularly difficult when deformable shapes are involved, and becomes even worse if the point sets are sparse. As a small number of knots leads to reasonable spline approximation of object boundaries, the paper considers a point-correspondence problem for sparse knot points of spline curves.

A. Point Correspondence

The general point correspondence problem is to find a match matrix *M* between two point sets, *A* and *B*, such that a cost function, consisted of a shape distance and a cost for outliers, is minimized. Outliers are points with no correspondence. Sets *A* and *B* may have different numbers of points, i.e., $A = \{A_j\}_{j=1}^{p}$ and $B = \{B_k\}_{k=1}^{r}$, and the match matrix $M = \{M_{j,k}\}_{j=1,k=1}^{j=p,k=r}$ is defined as follows

$$M_{j,k} = \begin{cases} 1 & \text{if point } A_j \text{ corresponds to point } B_k \\ 0 & \text{otherwise} \end{cases}$$

Typically, the shape distance $d_M(A,B)$ is defined as

$$d_M(A,B) = \frac{1}{|M|} \sum_{j=1}^{p} \sum_{k=1}^{r} M_{jk}\, d(A_j, B_k), \quad (8)$$

where $|M|$ is the number of 1's in *M*. In this paper, the cost of outliers is ignored if the matched points outnumber a minimum required number of pair.

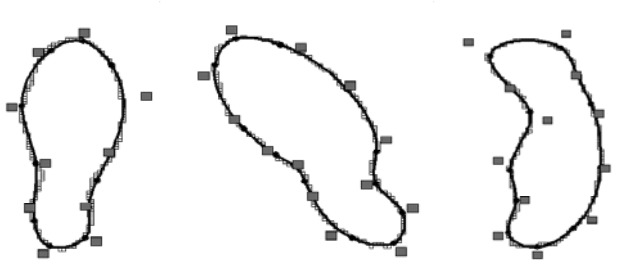

(a) (b) (c)

Figure 1. B-spline boundary representations for two affine-related objects (a-b) and a severely deformed object (c). Squares represent control points and small circles indicate knot points.

B. Corresponding Sparse Knots

Unfortunately, a B-spline curve is not uniquely described by a single set of control points. That is, with each different choice for the placement of the knot points, a different set of control points can be induced, but still describe the same curve. Thus, the direct comparison between their control points or knots is not appropriate for curve matching. Furthermore, in practical situations a few control points can represent outlines of most smooth objects, resulting in a small knot set that worsens the matching problem. To overcome this drawback in spline curve matching, and to apply direct comparison method, a careful rearrangement of knot position has been applied [16]. In this paper, the knot correspondence is formulated as a point correspondence problem with the match matrix having elements assigned as

$$m_{jk} = \exp\left(-d^2\left(A_j, B_k\right)/T - \left(\kappa_j^A - \kappa_k^B\right)^2\right) \qquad (9)$$

where a temperature variable T is used for deterministic annealing, which is described later section. The symbols κ_j^A and κ_k^B represent curvature of spline curves $\mathbf{f}_A(t)$ and $\mathbf{f}_B(s)$ at knot position j and k, respectively, and are defined as

$$\kappa = \left\|\dot{\mathbf{f}} \times \ddot{\mathbf{f}}\right\| / \left\|\dot{\mathbf{f}}\right\|^3 . \qquad (10)$$

Equation (9) incorporates both Euclidean distance and curvature at knot points, by which two geometrically different points would not match only because they are spatially close. This is similar to the "softassign" method in [20], but instead each element m_{jk} is discretized making the match matrix comply with the definition in previous section.

C. Thin Plate Spline Deformation Energy

The thin plate spline (TPS) is a commonly used basis function for representing coordinate mappings from a point set $\{\mathbf{v}_i = (x_i, y_i)\}_{i=0}^p$ to its corresponding points $\{\mathbf{v}_i' = (x_i', y_i')\}_{i=0}^p$ [4]. Here, the locations (x_i, y_i) must be all different and are not collinear. Then, the TPS interpolant $f(x, y)$ minimizes the bending energy

$$I_f = \iint_{\mathbb{R}^2} \left(f_{xx}^2 + 2f_{xy}^2 + f_{yy}^2\right) dxdy \qquad (11)$$

and has the form

$$f(x, y) = \mathbf{a}_1 + \mathbf{a}_x x + \mathbf{a}_y y + \sum_{i=1}^{p} \mathbf{w}_i U\left(\left\|(x_i, y_i) - (x, y)\right\|\right) \qquad (12)$$

where $U(r) = r^2 \log r$, and TPS coefficients $\mathbf{a}_1$, $\mathbf{a}_x$, $\mathbf{a}_y$, and $\mathbf{w}_i$ are 2×1 column vectors. Together with the interpolation conditions, $f(x_i, y_i) = (x_i', y_i')$, and other constraints on $\mathbf{w}_i$'s, this yields a linear system for the TPS coefficients:

$$\mathbf{L}\begin{bmatrix}\mathbf{w}_{p\times 2}\\ \mathbf{a}_{3\times 2}\end{bmatrix} = \begin{bmatrix}\mathbf{v}'_{p\times 2}\\ \mathbf{o}_{3\times 2}\end{bmatrix}, \qquad \mathbf{L} = \begin{bmatrix}\mathbf{K}_{p\times p} & \mathbf{P}_{p\times 3}\\ \mathbf{P}^T_{3\times p} & \mathbf{O}_{3\times 3}\end{bmatrix} \qquad (13)$$

where $K_{i,j} = U(\|(x_i, y_i) - (x_j, y_j)\|)$, the ith row of $\mathbf{P}$ is $(1, x_i, y_i)$, $\mathbf{a} = [\mathbf{a}_1 \quad \mathbf{a}_x \quad \mathbf{a}_y]^T$, $\mathbf{O}$ and $\mathbf{o}$ are zeros matrices, $\mathbf{w}$ and $\mathbf{v}'$ are formed from $\mathbf{w}_i$ and $\mathbf{v}_i'$, respectively. The subscripts indicate size of matrices. Then, the $\mathbf{L}$ is nonsingular, and the bending energy, sometimes called deformation energy, is proportional to

$$I_f \propto \mathbf{w}^T \mathbf{K} \mathbf{w} . \qquad (14)$$

When noise is present between the corresponding points, the exact interpolation condition is relaxed by introducing a regularization parameter λ, and the minimization problem is given

$$\xi(f) = \sum_{i=1}^{p} \left(\mathbf{v}_i' - f(x_i, y_i)\right)^2 + \lambda I_f . \qquad (15)$$

The λ controls the amount of smoothing; the limiting case of $\lambda = 0$ reduces to exact interpolation. The regularized case can be solved by simply replacing the matrix $\mathbf{K}$ by $\mathbf{K} + \lambda\mathbf{I}$, where $\mathbf{I}$ is the p×p identity matrix [23]. Since the regularization parameter λ is dependent on object scale, the size of objects is normalized to have maximum length of 1 and set λ to 1.

One drawback of the TPS model is that its solution requires the inversion of a large, dense matrix of size (p+3)×(p+3), where p is the number of points in the data set. However, the proposed curve-matching algorithm performs the correspondence search only for spline knot points, which is a small set compared to the number of data points. This means that the size of matrix $\mathbf{L}$ can be much smaller than typical cases.

D. Deterministic Annealing Method

TPS has been also used for point correspondence problems of non-rigid objects [1,6]. A popular technique in solving such a non-rigid problem is to use deterministic annealing method. At a given high value of temperature T, the match matrix is extracted by the equation (9). At this stage, the correspondence mostly depends on geometric information of object boundaries. Then, the TPS parameters are estimate based on the match matrix, and knot points are warped by the equation (12). As the temperature reduces, by which the correspondence becomes more relying on physical distance, the above procedure is repeated until M converges.

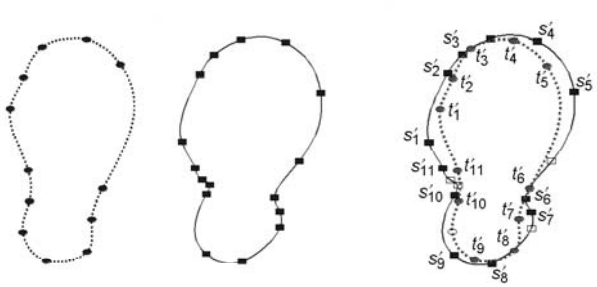

(a) Object A (b) Object B (c) Knot Correspondence

Figure 2. Example of sparse knot correspondence.

Figure 2 shows an example for knot correspondence. Object A is the same as in Figure 1a, and object B is an affine transformed version of one in Figure 1b. Affine parameters are estimated by the means presented in [16]. Figure 2c shows the resulting knot correspondence. Outliers are depicted as open circles and squares.

IV. COST FUNCTION AND MATCHING

Match matrix *M* estimated in the previous section gives us one-to-one correspondence between two sets of knot points of B-spline curves. Let $\mathbf{f}_A(t)$ be a *p*-knot periodic B-spline representation of curve *A* with knots $\{t_j\}_{j=1}^{p}$, and let $\mathbf{f}_B(s)$ be a similar representation of a curve *B*, having *r* knots $\{s_k\}_{k=1}^{r}$. Sets of knot points for each curve are calculated at each knot location and represented as $\{A_j = (x_j^A, y_j^A)\}_{j=1}^{p}$ and $\{B_k = (x_k^B, y_k^B)\}_{k=1}^{r}$. Then, the match matrix *M* represents the correspondence of a group of points in $\{A_j\}_{j=1}^{p}$ to a group of points in $\{B_k\}_{k=1}^{r}$, yielding new ordered knot locations: $\{t_k'\}_{k=1}^{p'}$ and $\{s_k'\}_{k=1}^{p'}$, so that intervals $[t_k', t_{k+1}')$ and $[s_k', s_{k+1}')$ represent matching portions in curve $\mathbf{f}_A(t)$ and $\mathbf{f}_B(s)$, respectively.

A matching cost function between curve *A* and *B*, $\xi(A,B)$, is a sum of total deformation energy, $\xi_d(A,B)$, and strain difference, $\xi_s(A,B)$, and defined as

$$\begin{aligned} \xi(A,B) &= \xi_d(A,B) + \xi_s(A,B) \\ \xi_d(A,B) &= \sum_l \mathbf{w}_l^T \mathbf{K}_l \mathbf{w}_l \\ \xi_s(A,B) &= \lambda_s \sum_{i=1}^{p'} \left(\mu^A \int_{t_i'}^{t_{i+1}'} \left(\kappa^A(t)\right)^2 dt - \mu^B \int_{s_i'}^{s_{i+1}'} \left(\kappa^B(s)\right)^2 ds \right)^2 \end{aligned} \tag{16}$$

where

$$\mu^A = \frac{(-1)^{C_i^A}}{t_{i+1}' - t_i'} \qquad \mu^B = \frac{(-1)^{C_i^B}}{s_{i+1}' - s_i'}$$

The total deformation energy penalizes high deformation when the curve *A* deforms onto the curve *B*. The deformation energy is calculated when searching the point correspondence as described in section III. If the deterministic annealing repeats *l* times, the total deformation energy is the sum of each deformation. The strain difference measures the geometric dissimilarity between two curves by the squared sum of difference of strain energy. For each portion, mean strain energy is used as the dissimilarity measure. Here, $t_{p'+1}' = t_1'$ and $s_{p'+1}' = s_1'$. A special care is required when $t_p \in [t_k', t_{k+1}')$ or $s_p \in [s_k', s_{k+1}')$ for $k = 1, \cdots, p'$. Convexity of curve segments is reflected in the parameters C_i^A and C_i^B, having 0 for convex and 1 for concave. The overall procedure is as follows:

1. Perform contour extraction from an image.
2. Fit periodic B-spline curve to the contour points.
3. Find corresponding knots between the extracted B-spline curve and a stored model.
4. Calculate the matching cost.
5. Repeat steps 3 and 4 for each stored model, and determine a model having the least cost (best match).

V. EXPERIMENTAL RESULTS

The proposed curve matching method has been tested successfully with three different datasets. First, a set of ivy leaves was arbitrarily affine transformed and then slightly deformed as shown in Figure 3. The outlines of the original leaves are depicted in the second row, and the outlines of the resulting deformed objects are shown in the next three rows. Original leaves are labeled L1 to L6, and the deformed objects are labeled D1 to D3. This dataset is used to measure the shape matching capability of the proposed method.

Matching costs defined in equation (16) are calculated for the dataset and summarized in Table 1. The first six columns of the table show matching costs between leaves, and the next three columns show matching costs between the originals and their deformed versions. The values in the table correspond to strain energy difference ξ_s, deformation energy ξ_d, and total cost $\xi(L_i, L_j)$, respectively. λ_s is set to 100 for all experiments presented here. The table shows that different shapes have high ξ_s and/or ξ_d, resulting in high total cost. The leaf pairs L1-L6, L2-L4, and L3-L5, however, are quite similar in shape and their matching costs are relatively low compared with other pairs. Meanwhile, the matching costs between an original leaf and its deformed outlines are noticeably low. This demonstrates the ability of the algorithm to recognize deformed shapes, by matching each one to its original.

The matching algorithm, which requires point correspondences between sparsely distributed spline knot points, relies substantially on initial alignment of two objects to be matched. One means of achieving initial alignment is with an affine parameter estimator that uses moments calculated from spline curves [16]. However, it has been experienced that the estimator is sensitive to noise and often comes up with poor results, especially for heavily transformed objects. To improve the capability of the same estimator, an initial rough alignment is provided by using the multilevel approximation capability of spline curves [15]. Since the incremental knot insertion method is used, the initial approximation curves resemble ellipses and shows global trends of object boundaries. Figures 4a and 4b show the fine (solid) and the coarse (dotted) spline approximations of L4 and its D1 form. Geometric relations such as rotation and scaling can be obtained by eigenanalysis of a few points

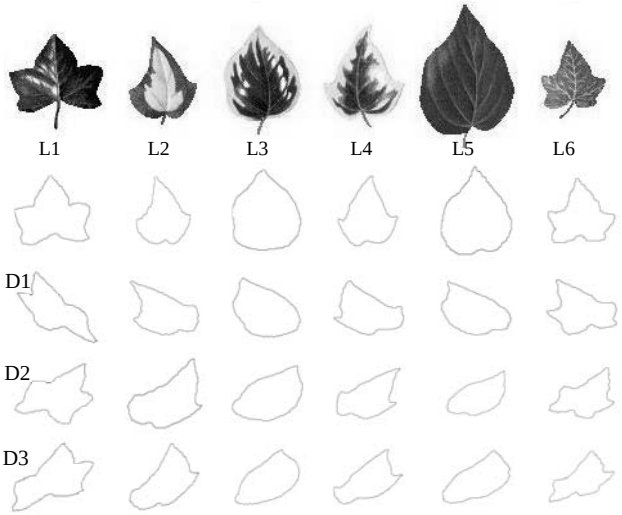

Figure 3. Ivy leaves dataset. The original leaves (L1 to L6) are affine transformed and then deformed to form D1 to D3. Scales of deformed objects are normalized for display purpose.

Table 1. Each cell shows matching cost. ξ_s, ξ_d, and $\xi(L_i, L_j)$. λ_c is set to 100.

	L1	L2	L3	L4	L5	L6	D1	D2	D3
L1	0	1.50 1.06 2.56	2.99 0.92 3.91	3.59 0.76 4.35	2.32 0.90 3.22	0.93 0.40 **1.33**	0.49 0.41 **0.90**	0.37 0.71 **1.08**	0.44 0.63 **1.07**
L2	1.40 1.17 2.57	0	1.09 1.51 2.60	0.44 0.66 **1.10**	1.56 1.79 3.35	1.31 0.75 2.06	0.32 0.67 **0.99**	0.37 0.54 **0.91**	0.33 0.30 **0.63**
L3	3.70 0.68 4.38	1.22 0.87 2.09	0	2.20 0.72 2.92	0.81 0.76 **1.57**	5.40 0.95 6.35	0.19 0.23 **0.42**	0.09 0.33 **0.42**	0.26 0.51 **0.77**
L4	3.36 0.97 4.33	1.83 0.09 **1.92**	2.51 0.69 3.20	0	3.00 0.77 3.77	2.36 0.55 2.91	0.47 0.61 **1.08**	0.21 0.89 **1.10**	0.43 0.46 **0.89**
L5	1.87 0.77 2.64	2.36 0.22 2.58	0.87 0.73 **1.60**	2.46 0.30 2.76	0	3.05 0.54 3.59	0.16 0.56 **0.72**	0.36 0.33 **0.69**	0.12 0.17 **0.29**
L6	1.20 0.79 **1.99**	2.22 0.76 2.98	4.29 1.58 5.87	2.66 0.90 3.56	4.13 1.00 5.13	0	0.46 0.62 **1.08**	0.51 0.55 **1.06**	0.57 0.61 **1.18**

sampled from the two coarse approximations. The finer-scale spline fit of D1 is rotated and scaled, and the result is shown in Figure 4c. With the rough alignment, affine parameters are estimated based on the method described in [15]. Figure 4d shows the final alignment. The figure also shows the knot correspondence with labels. Note that the correspondence does not solely depend on Euclidean distance and that instead curvature information leads to correct point matching.

The next experiment shows that the spline curve matching method is capable of model-based shape detection. For this experiment, an image that contains different shapes of blob as shown in Figure 5a is used. Let the spline curve depicted in Figure 5b be a model for matching. The model is simply a spline approximation of typical shape of interest, and contains a few knot points. Each blob is segmented from the image and its boundary is approximated with a spline curve. Matching results for selected blobs that are numbered in the image are shown in Figure 5c. Blobs numbered from B1 to B6 are correctly detected as matches to the model,

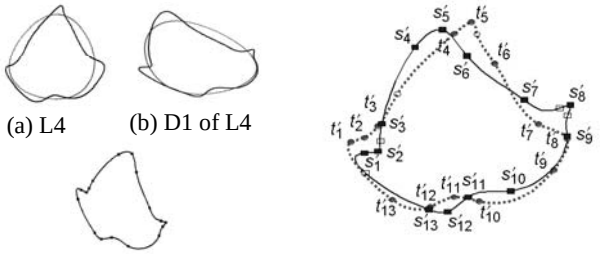

Figure 4. Alignment and point correspondence.

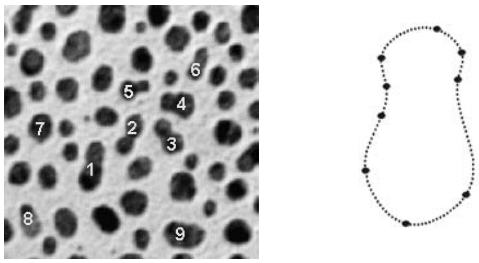

B1	B2	B3	B4	B5	B6	B7	B8	B9
0.32 0.21 **0.54**	0.38 0.43 **0.81**	0.22 0.44 **0.66**	0.23 0.17 **0.40**	0.07 0.11 **0.18**	0.13 0.06 **0.19**	1.45 0.59 2.04	1.92 0.13 2.05	0.96 0.32 1.28

(c) Matching cost

Figure 5. Model-based shape detection.

while the others have high matching costs. Blob B2 has a relatively high cost compared to other detected ones due to its slightly displaced indentations.

The last experiment demonstrates the ability of the proposed curve matching method to classify tree outlines. This is often performed manually as a means of evaluating the state of a tree's health. A reliable curve matching system could be used in tree health monitoring system. Tree outline models are depicted with their labels in the first two rows in Figure 6. Input tree images are segmented, and outlines are obtained automatically through spline fits by interpolating local convex points. Then the curve matching method is applied to determine which model outline is the best fit to each extracted tree outline. In the figure, tree outlines are represented with solid lines, and corresponding best-fit models are denoted with dotted line. It can be seen that appropriate outline models can be selected by using this matching method.

VI. CONCLUSION

This paper has presented a new curve matching method using sparse spline knot points. Corresponding knot points are first detected automatically. The system then calculates deformation energy and strain differences of the spline approximations. Despite sparse distributions of knot points, the experimental results show that the method is promising for shape detection and recognition. Because only a few knot points are used in the matching process, the algorithm is fast and is applicable to real-time tasks such as target detection, industrial robot vision, etc.

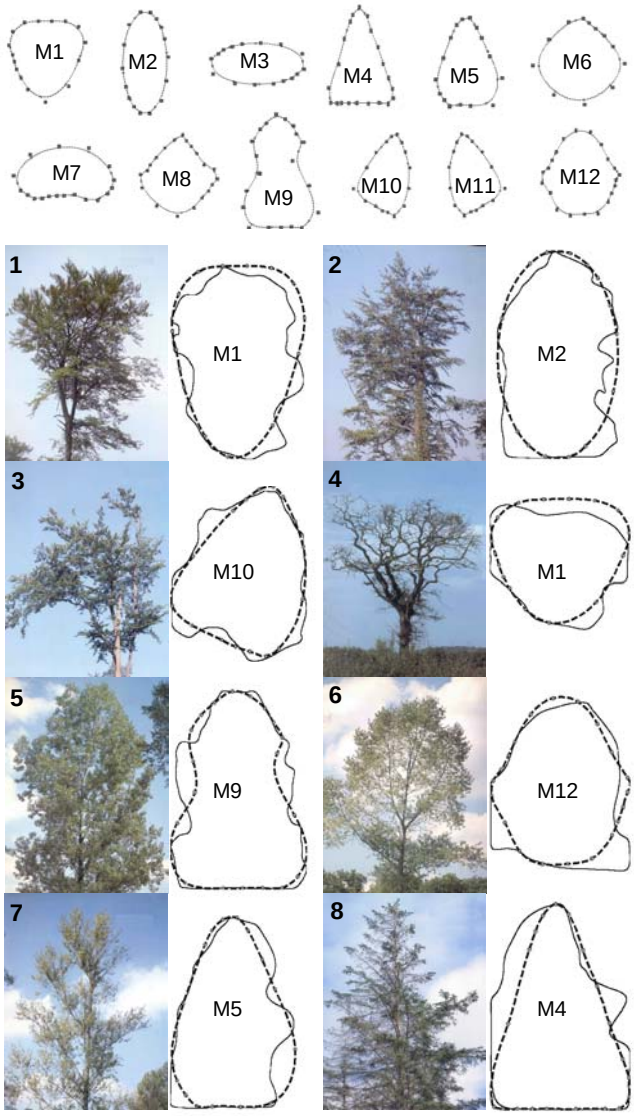

Figure 6. Model-based tree outline classification.

VII. REFERENCES

[1] A. Almansa and L. Cohen, "Fingerprint Image Matching by Minimization of a Thin-Plate Energy Using a Two-Step Algorithm with Auxiliary Variables", *5th IEEE Workshop on Applications of Computer Vision*, 2000, pp. 35-40.

[2] A. Amini, R. Curwen, and J. Gore, "Sankes and Splines for Tracking Non-Rigid Heart Motion", *European Conf. on Computer Vision*, Cambridge, U.K., 1996, pp.251-261.

[3] S. Belongie, J. Malik, and J. Puzicha, "Shape Matching and Object Recognition Using Shape Contexts", *IEEE Trans. on Pattern Analysis and Machine Intelligence*, vol. 24, no. 4, 2002, pp. 509-522.

[4] F.L. Bookstein, "Principal Warps: Thin-Plate Splines and the Decomposition of Deformations", *IEEE Trans. on Pattern Analysis and Machine Intelligence*, vol. 11, no. 6, June 1989, pp 567-585.

[5] P. Brigger, J. Hoeg, and M. Unser, "B-Spline Snakes: A Flexible Tool for Parametric Contour Detection", *IEEE Trans. on Image Processing*, vol.9, no.9, 2000, pp. 1484-96.

[6] H. Chui and A. Rangarajan, "A New Algorithm for Non-Rigid Point Matching", *IEEE Conf. on Computer Vision and Pattern Recognition*, vol. 2, 2000, pages 44-51.

[7] F.S. Cohen, Z. Huang, and Z. Yang, **"**Curve Recognition using B-spline Representation"**,** *IEEE Workshop on Applications of Computer Vision*, 1992, pp. 213-220.

[8] F.S. Cohen and J. Wang, "Part I: Modeling Image Curves Using Invariant 3-D Object Curve Models-A Path to 3-D Recognition and Shape Estimation from Image Contours", *IEEE Trans. on Pattern Analysis and Machine Intelligence*, vol. 16, no. 1, January 1994, pp. 1-12.

[9] P. Dierckx, *Curve and Surface Fitting with Splines*, Oxford University Press Inc., Oxford, U.K., 1993.

[10] N. Duta, M. Sonka, and A.K. Jain, "Learning Shape Models from Examples using Automatic Shape Clustering and Procrustes Analysis", *16th Intl. Conf. on Information Processing in Medical Imaging*, Hungary, 1999, pp. 370-5.

[11] G. Farin, *Curve and Surfaces for Computer Aided Geometrical Design*, San Diego, Academic Press, 1993.

[12] M.A.T. Figueiredo, J.M.N. Leitao, and A.L. Jain, "Unsupervised Contour Representation and Estimation Using B-Splines and a Minimum Description Length Criterion", *IEEE Trans. on Image Processing*, vol. 9, no. 6, 2000, pp. 1075-1087.

[13] M. Flickner, J. Hafner, E.J. Rodriguez, and J.L.C. Sanz, "Periodic Quasi-Orthogonal Spline Bases and Applications to Least-Squares Curve Fitting of Digital Images", *IEEE Trans. on Image Processing*, vol. 5, no. 1, 1996, pp. 71-88.

[14] Y. Gdalyahu and D. Weinshall, "Flexible Syntactic Matching of Curves and its Application to Automatic Hierarchical Classification of Silhouettes", *IEEE Trans. on Pattern Analysis and Machine Intelligence*, vol. 21, no. 12, December 1999, pp.1312-1328.

[15] Y. Gu and T. Tjahjadi, "Coarse-to-Fine Planar Object Identification Using Invariant Curve Features and B-Spline Modeling", *Pattern Recognition*, vol. 33, 2000, pp. 1411-22.

[16] Z. Huang and F.S Cohen, "Affine-Invariant B-Spline Moments for Curve Matching", *IEEE Trans. on Image Processing*, vol. 5, no. 10, 1996, pp. 1473-1480.

[17] A.K. Jain, Y. Zhong, and S. Lakshmanan, "Object Matching using Deformable Templates", *IEEE Trans. on Pattern Analysis and Machine Intelligence*, vol. 18, no. 3, 1996, pp. 267-278.

[18] M. Kass, A. Witkin, and D. Terzopoulos, "Snakes: Active Contour Models", *Intl. Journal of Computer Vision*, vol. 1, no. 4, 1988, pp. 321-331.

[19] S. Menet, P. Saint-Marc, and G. Medioni. "Active Contour Models: Overview, Implementation and Applications", *IEEE Conf. on Systems Management and Cybernetics*, 1990, pp. 194-199.

[20] A. Rangarajan, H. Chui, and F.L. Bookstein, "The Softassign Procrustes Matching Algorithm", *Information Processing in Medical Imaging*, James Duncan and Gene Gindi, eds., Springer, 1997, pages 29-42.

[21] D. Skea, I. Barrodale, R. Kuwahara, and R. Poeckert, "A Control Point Matching Algorithm", *Pattern Recognition*, vol. 26, 1993, pp. 269-276.

[22] H.J. Wolfson, "On Curve Matching", *IEEE Trans. on Pattern Analysis and Machine Intelligence*, vol. 12, Issue 5, May 1990, pp. 483 –489.

[23] G. Wahba, *Spline Models for Observational Data*, SIAM, 1990.

IECON'03

The 29th Annual Conference
Of The IEEE Industrial Electronics Society

Hotel Roanoke and Conference Center, Roanoke, Virginia, USA
November 2nd (Sunday) to Thursday, November 6th (Thursday) 2003

Sponsored by IEEE Industrial Electronics Society

Technical Co-Sponsors:

SICE – Society of Instrumentation and Control Engineers
Virginia Tech – Center for Organizational and Technological Advancement

IECON'03: The 29th Annual Conference of the IEEE Industrial Electronics Society

IEEE Catalog Number 03CH37468

ISBN: 0-7803-7906-3

Library of Congress: 2003103877

Additional copies can be ordered from

IEEE Service Center
445 Hoes Lane
Piscataway, NJ 08854

1-800-678-IEEE
1-732-981-1393
1-732-981-1721 (FAX)